



Anomalous Soft Non-Euclidean Springs

Ido Levin and Eran Sharon*

Racah Institute of Physics, The Hebrew University, Jerusalem 91904, Israel

(Received 20 September 2015; published 20 January 2016)

In this work we study the mechanical properties of a frustrated elastic ribbon spring—the non-Euclidean minimal spring. This spring belongs to the family of non-Euclidean plates: it has no spontaneous curvature, but its lateral intrinsic geometry is described by a non-Euclidean reference metric. The reference metric of the minimal spring is hyperbolic, and can be embedded as a minimal surface. We argue that the existence of a continuous set of such isometric minimal surfaces with different extensions leads to a complete degeneracy of the bulk elastic energy of the minimal spring under elongation. This degeneracy is removed only by boundary layer effects. As a result, the mechanical properties of the minimal spring are unusual: the spring is ultrasoft with a rigidity that depends on the thickness t as $t^{7/2}$ and does not explicitly depend on the ribbon's width. Moreover, we show that as the ribbon is widened, the rigidity may even decrease. These predictions are confirmed by a numerical study of a constrained spring. This work is the first to address the unusual mechanical properties of constrained non-Euclidean elastic objects.

DOI: [10.1103/PhysRevLett.116.035502](https://doi.org/10.1103/PhysRevLett.116.035502)

In recent years there has been an extensive study of the equilibrium configurations of prestrained elastic plates. These plates, also known as non-Euclidean plates (NEPs) can be generated via growth, plastic deformation, or active swelling, which are nonuniform across the sheet. Within the formalism of incompatible elasticity such nonuniform deformation fields prescribe non-Euclidean reference metric fields $\bar{\mathbf{a}}$ on the plate. The elastic strain is defined with respect to $\bar{\mathbf{a}}$. Non-Euclidean plates were shown to adopt nontrivial 3D configurations, when free of external stresses [1–6]. This tendency, which stems from their geometrical frustration, was pointed out as a desired property for the design of self-shaping bodies. However, until now no attention was paid to the mechanical behavior of NEPs under an external load. In this work we perform the first study of the mechanics of a loaded non-Euclidean plate, showing how its frustration leads to some remarkable properties that are absolutely excluded from ordinary, compatible, elastic bodies.

Constraining compatible plates and shells perturbs both the stretching and bending energies around their minima. Contrarily, the configuration of a free frustrated thin NEP is close to an embedding of its reference metric, far from the minimum of the bending energy. Therefore, when slightly constraining a thin NEP, the bending energy is not perturbed around its minimum, a fact that can have unusual mechanical consequences. We demonstrate such unusual mechanics by studying a new kind of an incompatible ribbon spring—a ribbon with a reference metric of a minimal surface [non-Euclidean minimal spring (NEMS)]. We analyze the dominant energy terms of a stretched NEMS showing the complete degeneracy of its bulk energy under extension. This degeneracy is removed only by boundary layer effects, leading to an anomalous flexibility of the spring. In addition,

we show that in some cases the rigidity of the spring decreases as its width is increased. All these unusual properties are confirmed by a numerical study.

Ribbon springs, springs that are made of curled elastic strips, are common elements in engineering applications. Frequently, they appear in biological systems [7,8] and as products of self-assembly processes in the nanoscale [9–12]. Such springs undergo various mechanical instabilities [13] and have complex mechanical properties, such as a highly nonlinear force-extension relation that comprises hysteresis [14,15]. Most such springs are ribbons with a single spontaneous curvature (in this work we use the term “reference curvature”); i.e., they can be viewed as being cut from a cylindrical shell. The rigidity of these springs results from the accumulation of elastic energy upon elongation or shortening of the spring. Thin enough ribbon springs contain only negligible in-plane strains. Therefore, their elastic energy is dominated by the bending energy and their rigidity κ typically scales as $\kappa \propto (YWk^2t^3/L)$ [15]. Here, t , W , L , k , and Y are the thickness, width, length, reference curvature, and Young's modulus of the ribbon, respectively.

More complicated ribbon springs, which have double reference curvature, are known to be created via self-assembly processes or by the growth of biological tissues. Such ribbon springs are geometrically incompatible and undergo nontrivial shape transitions [16,17]. Still, their rigidity stems from deviations of the curvature tensor from its reference values and, as such, scales similarly to the rigidity of ordinary ribbon springs.

It was recently shown that NEPs can form ribbon springs. For example, consider a thin and narrow elastic strip ($t \ll W \ll L$) with margins that are longer than its interior. Such ribbons are generated via the nonuniform

lateral growth or swelling of macroscopic strips [18], and appear also as nanoribbons [19]. A recent study of such unconstrained non-Euclidean ribbons showed that they take springlike configurations despite the absence of a reference curvature [20].

The mechanics of non-Euclidean ribbons can be studied within the framework of incompatible elasticity [5]. In this formalism, any given configuration of a ribbon is accompanied with two tensors: the actual metric tensor \mathbf{a} and the actual curvature tensor \mathbf{b} . The elastic energy of such ribbons can be separated into two terms, stretching and bending, that depend on deviations of \mathbf{a} from $\bar{\mathbf{a}}$ and \mathbf{b} from zero, respectively:

$$E = tE_S + t^3E_B. \quad (1)$$

Here,

$$E_S \propto Y \int [(1-\nu)\text{Tr}(\bar{\mathbf{a}} - \mathbf{a})^2 + \nu\text{Tr}^2(\bar{\mathbf{a}} - \mathbf{a})] dS$$

and

$$E_B \propto Y \int [(1-\nu)\text{Tr}\mathbf{b}^2 + \nu\text{Tr}^2\mathbf{b}] dS$$

are the stretching and bending contents, respectively, where Y and ν are the Young's modulus and Poisson ratio, respectively, and $dS = \sqrt{\det \bar{\mathbf{a}}} du dv$ is the intrinsic area measure. When $\bar{\mathbf{a}}$ is nonflat (the reference Gaussian curvature associated with it, via Gauss's *Theorema Egregium*, satisfies $\bar{K} \neq 0$), these two terms are incompatible: the elastic energy does not vanish in any configuration, and equilibrium configurations are set by the competition between the bending and stretching terms.

Some properties of incompatible elastic sheets can be deduced from simple geometrical arguments: based on the different scaling of the two energy terms, one can suggest that thin enough ribbons will favor stretch-free configurations, that is, embeddings of $\bar{\mathbf{a}}$. One can go further and show that if there exist embeddings of $\bar{\mathbf{a}}$ with finite bending content, the limit configuration at $t \rightarrow 0$ will be the bending minimizing embedding of $\bar{\mathbf{a}}$ [21]. Then, the elastic energy takes the form [5]

$$E \approx t^3 E_B = t^3 \frac{Y}{24(1+\nu)} \int \left(\frac{4H^2}{1-\nu} - 2\bar{K} \right) dS, \quad (2)$$

where H is the mean curvature of the configuration, under the constraint $K = \bar{K}$. Therefore, the bending minimizing embedding is the one that minimizes $\int |H| dS$ under this constraint.

The specific NEP we consider in this work is a non-Euclidean minimal spring—a non-Euclidean ribbon with a reference metric of a helicoid. This metric can be written as

$$\bar{\mathbf{a}} = \begin{pmatrix} \bar{p}^2 & 0 \\ 0 & \bar{p}k^{-1} \end{pmatrix}, \quad k = \frac{\bar{p}^{-1}}{1 + (\bar{R} + v)^2}, \quad (3)$$

where \bar{p} is its only length scale, which can arbitrarily be set to 1. Here, $v_{\min} \leq v \leq v_{\max}$ is the radial coordinate and \bar{R} is the radius at $v = 0$. The width of the ribbon is defined intrinsically, i.e., $W = v_{\max} - v_{\min}$ and its reference Gaussian curvature is given by $\bar{K} = -k^2$.

When considering a set of configurations of a stretched NEMS we recall that a catenoid can be continuously deformed into a helicoid [22]. Members of the helicoid-catenoid family (HCF) [22] are all helical, and are characterized by their pitch $0 \leq p \leq 1$ (Fig. 1). Interestingly, all the members of the HCF are isometric, implying that a catenoidlike NEMS can be extended all the way to a helicoid while keeping $\mathbf{a} = \bar{\mathbf{a}}$, i.e., without stretching. Moreover, all the members of this family are minimal surfaces, having a zero mean curvature [22]; i.e., they are embeddings of $\bar{\mathbf{a}}$, having the absolute minimum bending content. Therefore, the pitch p of a NEMS can be varied between 0 and 1 while simultaneously keeping the zero stretching condition $\mathbf{a}(p) = \bar{\mathbf{a}}$ and the minimal bending condition $H(p) = 0$. The bulk elastic energy, as it appears in Eq. (2), is therefore degenerate with respect to changes in p . That is, elongating or compressing the helical ribbon does not change its bulk energy.

The apparent degeneracy with respect to p is removed only by boundary layer effects. These can be estimated via global geometric considerations as well. A more elaborate study shows that for any finite thickness, the real energy-minimizing configuration of a NEP is not an exact embedding of $\bar{\mathbf{a}}$. It was shown that narrow boundary layers appear along the ribbon's edges [23]. Within these layers, the component of the curvature perpendicular to the edge, k_{\perp} , is decreased. (Note that when solving the equilibrium equations of forces and torques in the sheet, this condition appears as the imposed zero normal torque boundary condition). The scaling of the width of these boundary layers is

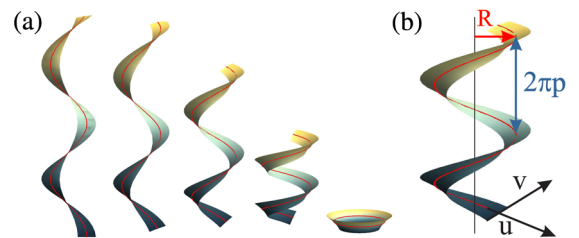


FIG. 1. A realization of the HCF. (a) An example of a few members of the HCF. These embeddings have pitch values of $p = 1, 0.9, 0.7, 0.4, 0$ (left to right). The number of turns is conserved under this transformation. The red curve in each surface is the midline, which is a helix with a radius $R = \sqrt{\bar{R}^2 + 1 - p^2}$. (b) A detailed example of an embedding with $p = 0.4$. The radial and azimuthal coordinates (v and u , respectively) are denoted along with the radius R and the pitch p .

$$W_b \propto t^{1/2} k_{\perp}^{-(1/2)}. \quad (4)$$

For thin sheets, this effect is small and is usually neglected. However, for a NEMS, the two commonly dominant energy terms are degenerate; hence, it is this weak effect that gives it its rigidity. It is straightforward to show that for HCF surfaces

$$k_{\perp} = k_0 \sqrt{1 - p^2}, \quad (5)$$

where k_0 is the value of k on the edge. Therefore, as the pitch is increased, k_{\perp} approaches zero and the boundary layers become less effective, leading to an increase in the ribbon's energy. It follows from Eqs. (2) and (4) that the reduction in the elastic energy within the boundary layer scales as $t^{7/2} k_0^{3/2}$. This scaling law of the energy sets the rigidity of the minimal spring. Since the rigidity stems from variations only within the boundary layer, it does not depend explicitly on the ribbon's width.

Consequently, the energy depends on the pitch, but with an anomalous scaling law

$$\begin{aligned} E(p) &\propto t^{7/2} \left(k_{\text{in}}^{3/2} + k_{\text{out}}^{3/2} \right) \left((1-\nu)p^2 + 1 + \nu \right)^{5/4} + E_0 \\ &\approx \left[(1+\nu)^{5/4} + \frac{5}{4}(1-\nu)(1+\nu)^{1/4} p^2 + \frac{5(1-\nu)^2}{32(1+\nu)^{3/4}} p^4 \right] \\ &\quad \times t^{7/2} \left(k_{\text{in}}^{3/2} + k_{\text{out}}^{3/2} \right) + E_0, \end{aligned} \quad (6)$$

where E_0 is the degenerate bulk energy, and k_{in} and k_{out} are the values of k_0 on the inner and outer edges, respectively. Looking at this expression, three anomalous properties of NEMSs become clear. The rigidity of such springs scales as $\kappa \propto t^{7/2}$, a higher power of t than for regular ribbon springs. Therefore, the minimal springs are ultrasoft. In addition, there is no explicit dependence of the energy on the ribbon's width W . This leads to the conjecture that springs of different widths have the same rigidity. This means, for instance, that cutting such a spring along the midline will result in two springs, each with a rigidity similar to that of the original one. In fact, as shown below, the rigidity might even slightly decrease when the ribbon's width is increased. Such an unusual property is a direct result of the fact that the bulk energy of the configurations of different pitch values is degenerate. Finally, Eq. (6) indicates the extended linearity of NEMSs. For $\nu = \frac{1}{2}$ the ratio between the coefficients of the quartic terms and the quadratic terms is $\frac{1}{24}$ compared to $\frac{1}{4}$ for the equivalent coefficients of a simple ribbon spring (see the Supplemental Material [24]).

In order to verify these predictions numerically, we perform a simulation of a constrained NEMS—minimizing Eq. (1) on a one-dimensional grid (see the Supplemental Material [24]). We exploit the helical symmetry of the elastic problem to reduce the dimensionality of the

simulation domain, finding the optimal radial profile for a given pitch.

We find that in the bulk, the configurations remain close to the relevant embeddings of $\bar{\mathbf{a}}$ (the relevant HCF member), having vanishing bulk stretching energy, while deviations from $\bar{\mathbf{a}}$ are confined to the boundary layers (Fig. 2). As discussed earlier, the magnitude of each boundary layer depends on the pitch. It is most significant at $p = 0$ (Fig. 2, square symbols) and disappears at $p = 1$ (circles). In order to estimate the bending energy on the edge, it is sufficient to find the value of k_{\perp} by minimizing the integrand in Eq. (2) [25], leading to $k_{\perp} = -\nu k_0 \sqrt{1 - p^2}$. For the catenoid, k_{\perp} coincides with one of the principal reference curvatures; hence, the bending energy on the edges is reduced by a factor of $1 + \nu/2$ (see the Supplemental Material [24]). This factor increases with p , approaching 1 for $p = 1$. These predictions are quantitatively confirmed (Fig. 2, inset).

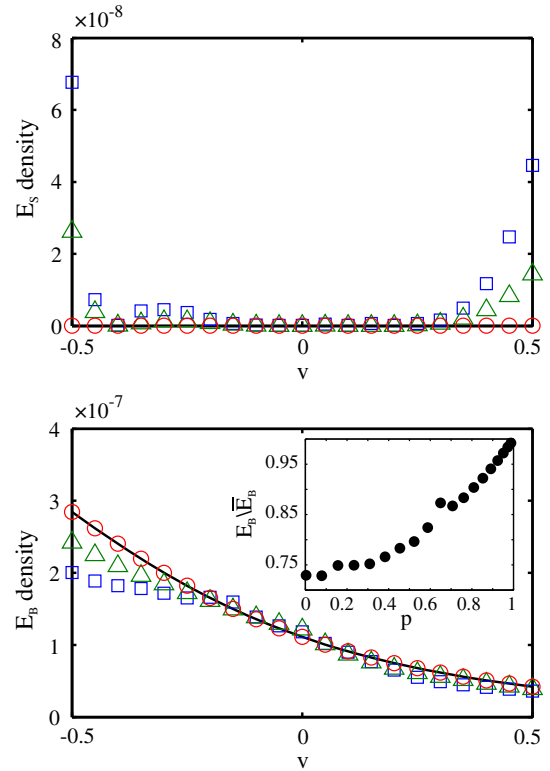


FIG. 2. The stretching (top) and bending (bottom) energy densities as functions of v , the radial coordinate, for different values of p ($p = 1$, circles; $p = 0.7$, triangles; $p = 0$, squares—see the configurations in Fig. 1). The energy densities are plotted in dimensionless units, that is, normalized by $Y\bar{p}$. The bending energy density of an isometric embedding is indicated (black line at the bottom panel). Both the inner and outer boundary layers are apparent for the lower pitch values and disappear for $p = 1$. As predicted, the ratio between the measured bending energy densities on the edges and those of the isometric embedding is 1 for $p = 1$ and approaches $\frac{3}{4}$ for $p \rightarrow 0$ (inset of the bottom panel). These results were obtained for $t = 0.02$, $W = 1$, and $\bar{R} = 1$.

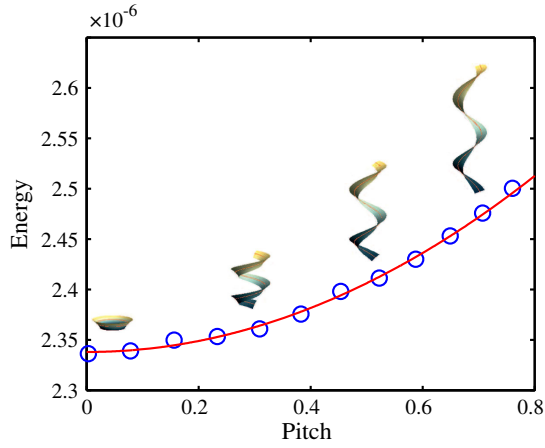


FIG. 3. The dimensionless energy ($E/Y\bar{p}^3$) of a minimal spring as a function of the pitch p (here, $t = 0.05$, $W = 1$). The data are well fitted by a parabola (red curve) in the entire range of deformation. The helical figures illustrate embeddings of $\bar{\mathbf{a}}$ with the relevant different pitch values.

The global minimum of the energy is obtained for $p = 0$ as predicted, and the energetic cost of the spring elongation is quadratic to a high degree in the regime $0 < p < 0.8$ (Fig. 3).

Hence, the rigidity κ of the ribbon is well defined by fitting a parabola to the energy. Measurements of κ for ribbons of different thickness confirm the predicted ultra-soft power law of $\kappa \propto t^{7/2}$ (Fig. 4).

In order to verify the prediction that the rigidity does not depend on the ribbon's width, we compute the rigidity

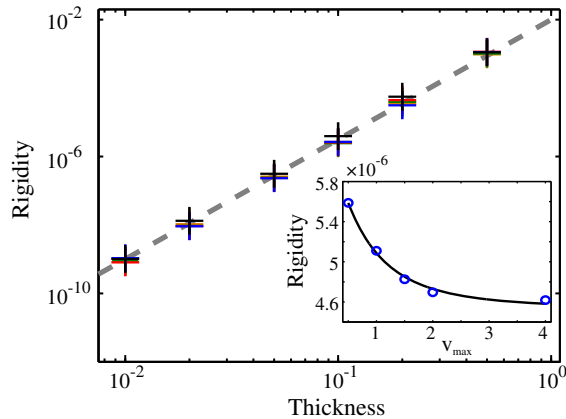


FIG. 4. Main graph: the dimensionless rigidity ($\kappa/Y\bar{p}$) of a minimal spring as a function of thickness for five different widths (in the range $1.4 < W < 4.6$). The data collapse to a single $t^{7/2}$ power law (gray dashed line). The data sets override each other, which is consistent with the prediction that the rigidity depends very weakly on the width. Inset: the rigidity as a function of v_{\max} , the outer radius, for $t = 0.1$ and $v_{\min} = 0.5$. The data indicate that widening the ribbon outwards leads to a decrease of the rigidity. The variation in the rigidity is well fitted by the predicted relation $\kappa \propto [1/1 + (\bar{R} + v_{\max})^2]^{3/2} + \text{const}$ (black solid line). For large widths ($v_{\max} \gg \bar{R}$), the rigidity is virtually constant.

versus the thickness for different values of W . The rigidities of NEMSs of different widths are indeed nearly indistinguishable (Fig. 4, main graph). A more detailed analysis shows that in fact there is a small variation of the rigidity with the width. Surprisingly, the rigidity is a decreasing function of the width; i.e., wider springs are softer than narrow ones (Fig. 4, inset). This counterintuitive property, which cannot occur in compatible springs, can be explained quantitatively. The elastic energy in the boundary layers scales as $k_0^{3/2}$, where for HCF surfaces it is given by Eq. (3). Therefore, increasing the outer radius v_{\max} will cause the rigidity to decrease: $\kappa \propto k_0^{3/2} + \text{const} = [1/1 + (\bar{R} + v_{\max})^2]^{3/2} + \text{const}$, where the constant stands for the contribution of the inner boundary layer. Our data present a good agreement with those predictions (Fig. 4, inset). For large widths, the constant contribution dominates κ , as predicted.

This study highlights the unusual mechanical properties of incompatible elastic sheets under constraints. These unusual properties result directly from geometrical incompatibility. In non-Euclidean sheets only a reference metric is determined, rather than a configuration; thus, they usually have a wide and shallow energy landscape. This allows relatively soft deformations between configurations that differ mainly in their bending energy [6]. In the unique case of the non-Euclidean minimal spring, both the stretching and bending bulk terms of the energy are completely degenerate over any equilibrium configuration. By addressing the hierarchy of the energy terms, i.e., stretching energy, bending energy, and boundary layer energy, we derived quantitative predictions for these unusual mechanical properties. These predictions were confirmed by a numerical study and the first experimental realizations of non-Euclidean minimal springs were constructed from selectively cross-linked responsive gels (see the Supplemental Material [24]). It is very likely that further study of other cases of constrained non-Euclidean plates will reveal mechanical structures with surprising properties. Such structures are not yet used in man made constructs, but are likely to appear naturally in biological and chemical systems.

This work was funded by European Research Council, SoftGrowth project.

*erans@mail.huji.ac.il

- [1] E. Sharon, B. Roman, M. Marder, G.-S. Shin, and H. L. Swinney, *Nature (London)* **419**, 579 (2002).
- [2] Y. Klein, E. Efrati, and E. Sharon, *Science* **315**, 1116 (2007).
- [3] Y. Klein, S. Venkataramani, and E. Sharon, *Phys. Rev. Lett.* **106**, 118303 (2011).
- [4] J. Kim, J. A. Hanna, M. Byun, C. D. Santangelo, and R. C. Hayward, *Science* **335**, 1201 (2012).

- [5] E. Efrati, E. Sharon, and R. Kupferman, *J. Mech. Phys. Solids* **57**, 762 (2009).
- [6] C. D. Santangelo, *Europhys. Lett.* **86**, 34003 (2009).
- [7] A. Fahn and M. Zohary, *Phytomorphology (Delhi)* **5**, 99 (1955).
- [8] S. Armon, E. Efrati, R. Kupferman, and E. Sharon, *Science* **333**, 1726 (2011).
- [9] F. Konikoff, D. Chung, J. Donovan, and M. Carey, *J. Clin. Invest.* **90**, 1155 (1992).
- [10] R. Oda, I. Huc, M. Schmutz, S. J. Candau, and F. C. MacKintosh, *Nature (London)* **399**, 566 (1999).
- [11] A. Singh, E. M. Wong, and J. M. Schnur, *Langmuir* **19**, 1888 (2003).
- [12] L. Ziserman, H.-Y. Lee, S. R. Raghavan, A. Mor, and D. Danino, *J. Am. Chem. Soc.* **133**, 2511 (2011).
- [13] J. Chopin, V. Démary, and B. Davidovitch, *J. Elast.* **119**, 137 (2015).
- [14] A. Goriely and P. Shipman, *Phys. Rev. E* **61**, 4508 (2000).
- [15] E. Starostin and G. van der Heijden, *Phys. Rev. Lett.* **101**, 084301 (2008).
- [16] S. Armon, H. Aharoni, M. Moshe, and E. Sharon, *Soft Matter* **10**, 2733 (2014).
- [17] Z. Chen, C. Majidi, D. J. Srolovitz, and M. Haataja, *Appl. Phys. Lett.* **98**, 011906 (2011).
- [18] J. Dervaux and M. Ben Amar, *Phys. Rev. Lett.* **101**, 068101 (2008).
- [19] V. B. Shenoy, C. D. Reddy, and Y.-W. Zhang, *ACS Nano* **4**, 4840 (2010).
- [20] E. Efrati, E. Sharon, and R. Kupferman, *Phys. Rev. E* **83**, 046602 (2011).
- [21] M. Lewicka and M. Reza Pakzad, *ESAIM Control Optim. Calc. Var.* **17**, 1158 (2011).
- [22] B. O'Neill, *Elementary Differential Geometry*, Revised 2nd ed., Elementary Differential Geometry Series (Academic Press, New York, 2006).
- [23] E. Efrati, E. Sharon, and R. Kupferman, *Phys. Rev. E* **80**, 016602 (2009).
- [24] See Supplemental Material at <http://link.aps.org/supplemental/10.1103/PhysRevLett.116.035502> for the analytical and numerical analysis and also preliminary experimental results.
- [25] This condition is completely equivalent to the boundary conditions imposed in order to obtain zero torque on a free edge, when solving the elasticity differential equation.